

DFT study of the structural and redox properties of $[\text{Cp}_2\text{Fe}_2\text{S}_4]^q$ complexes ($q = 0, +2, +1$ and -2)

Sophie Blasco,^a Isabelle Demachy,^a Yves Jean^{*a} and Agusti Lledos^{*b}

^a Laboratoire de Chimie-Physique (CNRS UMR 8000), Université Paris-Sud, 91405 Orsay cedex, France. E-mail: jean@lcp.u-psud.fr

^b Departament de Química, Universitat Autònoma de Barcelona, 08193 Bellaterra, Catalonia, Spain. E-mail: agusti@klingon.uab.es

Received (in Montpellier, France) 14th December 2000, Accepted 24th January 2001

First published as an Advance Article on the web 20th March 2001

Geometry optimisation of $[\text{Cp}_2\text{Fe}_2\text{S}_4]^q$ complexes ($q = 0, +2, +1$ and -2) has been performed using DFT calculations with the B3LYP functional. The theoretical structures of the neutral (two isomers) and the dicationic complexes are in satisfactory agreement with the X-ray data. Structures are proposed for the monocationic and the dianionic species observed in cyclic voltammetry experiments. Free solvation energies have been computed by means of PCM calculations and used to evaluate the redox potentials of the M^+/M , M^{2+}/M^+ and M/M^{2-} couples in dichloromethane and acetonitrile.

A large number of bimetallic complexes of the $\text{Cp}_2\text{M}_2\text{S}_4$ type have been synthesized and structurally characterized. These compounds are interesting for both their reactivity and their structural properties. They have been used as building blocks for the synthesis of metal–sulfur clusters,^{1,2} with a particular interest for cubane-type complexes³ owing to their relevance to metalloenzymes. On the other hand, these compounds exhibit a large variety of structures:¹ depending on the nature of the metal (Ti,⁴ V,⁵ Cr,⁶ Mo,^{7–9} Fe,^{10–15} Ru,¹⁶ Co¹³), the S_4 unit may involve terminal or bridged sulfur ligands and/or disulfur bridging ligands with a $\mu\text{-}\eta^1$, $\mu\text{-}\eta^2$ or $\mu\text{-}(\eta^1, \eta^2)$ coordination mode.

In this context, binuclear $\text{Cp}_2\text{Fe}_2\text{S}_4$ complexes have been used as starting materials for building up polynuclear iron–sulfur clusters,^{2,17} in particular the tetranuclear cluster because of the importance of the cubic Fe_4S_4 core for biological systems.² The iron complexes also nicely illustrate the versatile structural properties of this family of compounds. Two isomers (A and B) have been characterized for the neutral complex, with $(\mu\text{-}\eta^1\text{-S}_2, \mu\text{-}\eta^2\text{-S}_2)^{11–13}$ and $2[\mu\text{-}(\eta^2, \eta^1)\text{-S}_2]^{12}$ coordination modes of the S_2 units, respectively (Fig. 1). These isomers also seem to differ in the $\text{Fe}\cdots\text{Fe}$ interaction. In the former, the iron–iron distance (3.494 Å) rules out any interaction, while the distance of 2.650 Å in the latter is consistent with an iron–iron bonding interaction.¹² A dramatic structural change has been observed accompanying the double electrochemical oxidation of the $\text{Cp}^*\text{Fe}_2\text{S}_4$ complex: both disulfur ligands are coordinated in an (η^2, η^2) fashion in the dication (Fig. 1),^{14,15} with the $\text{Fe}\cdots\text{Fe}$ distance of 2.857 Å suggesting the absence of an Fe–Fe bond. On the other hand, both the neutral¹¹ and the dicationic¹⁴ species have been found to be *diamagnetic*. Electrochemical investigations on $\text{Cp}^*\text{Fe}_2\text{S}_4$ (isomer A) have also revealed the existence of an intermediate monocation in the double oxidation process.^{14,15} The reversibility of the one-electron oxidation reaction suggested that the $\mu\text{-}\eta^1 \rightarrow \mu\text{-}\eta^2$ ligand reorientation did not occur in this step; that is, the structure of the monocation resembles that of the neutral compound.¹⁵ The formation of the dianionic species through a single irreversible two-electron reduction of the neutral isomer A has also been observed. Its structure is still unknown, but cleavage of the S–S bond in the $\eta^2\text{-S}_2$ ligand has been proposed.¹⁵

From a theoretical point of view, some of the electronic factors at work for stabilizing one or other of the isomers in the $\text{M}_2\text{Cp}_2\text{S}_4$ compounds have been explored at the extended Hückel level for the $\text{Mo}_2\text{Cp}_2\text{S}_4$ complex.¹⁸ More recently, quantitative calculations on the structure and the reactivity of bimetallic complexes have become feasible, most of them using density functional theory. Among the most recent related studies are those of complexes with an O_2 unit bridged in $(\mu\text{-O})_2$, $\mu\text{-}\eta^1\text{-O}_2$ or $\mu\text{-}\eta^2\text{-O}_2$ fashions¹⁹ and the study of the interconversion between $(\mu\text{-O})_2$ and $\mu\text{-}\eta^2\text{-O}_2$ coordination modes in the $\text{Cu}_2\text{O}_2(\text{NH}_3)_6^{2+}$ complex.^{19e} A bimetallic compound with a bridging “ O_4 ” unit involving a dioxygen and two oxo ligands, $[\text{Mn}_2(\mu\text{-O})_2(\mu\text{-}\eta^1\text{-O}_2)(\text{NH}_3)_6]^{z+}$ with $z = 0, 2, 4$, has also been studied in various electronic states.²⁰ Calculations on metal–sulfur compounds are less numerous and involve $[\text{Fe}_2\text{S}_2(\text{SR})_4]^{z-}$ ($z = 2, 3$) inorganic iron complexes with a $(\mu\text{-S})_2$ coordination mode of the sulfur ligands.²¹ To our knowledge, no quantitative calculations have yet been reported on the family of organometallic complexes of the $\text{Cp}_2\text{M}_2\text{S}_4$ type.

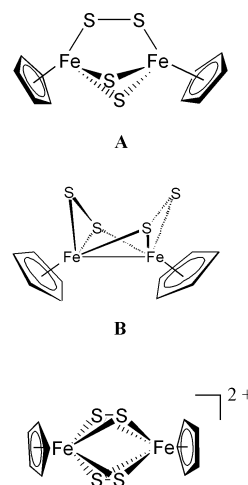


Fig. 1 Schematic drawings of the structure of the neutral complexes $\text{Cp}_2\text{Fe}_2(\mu\text{-}\eta^1\text{-S}_2)(\mu\text{-}\eta^2\text{-S}_2)$ (isomer A) and $\text{Cp}_2\text{Fe}_2[\mu\text{-}(\eta^1, \eta^2)\text{-S}_2]_2$ (isomer B) and the dicationic species $\text{Cp}^*_2\text{Fe}_2(\mu\text{-}\eta^2\text{-S}_2)_2^{2+}$ (bottom).

In this paper studies, by means of DFT calculations, of the bimetallic $[\text{Cp}_2\text{Fe}_2\text{S}_4]^q$ complexes ($q = 0, +1, +2$ and -2) are reported. Full geometry optimizations were performed for the singlet state of the neutral, dicationic and dianionic species, and for the lowest doublet state of the monocationic complex. All the stationary points located on the potential energy surface were further characterized. For the neutral and the dicationic complexes, the geometrical and energetic results are compared to the available experimental data while predictions are made for the structure of the monocationic and dianionic species. Finally, free energies of solvation of these species were calculated in order to evaluate the energetics of the redox processes.

Computational details

Calculations were performed with the GAUSSIAN 98 series of programs.²² Density functional theory (DFT)^{23,24} was applied with the B3LYP functional.^{25–27} A quasirelativistic effective core potential operator was used to represent the 10 innermost electrons of the iron atom²⁸ as well as the electron core of S atoms.²⁹ The basis set for the metal was that associated with the pseudopotential,²⁸ with a standard double- ζ LANL2DZ contraction.²² The basis set for the S atoms was that associated with the pseudopotential,²⁹ with a standard double- ζ LANL1DZ contraction²² supplemented with a set of d-polarization functions.³⁰ A 6-31G basis set was used for the C and H atoms.³¹ Solvent effects were taken into account by means of polarized continuum model (PCM) calculations³² using standard options of PCM and cavity keywords.²² Free energies of solvation were calculated with CH_3CN ($\epsilon = 36.64$), CH_2Cl_2 ($\epsilon = 8.93$) and THF ($\epsilon = 7.58$) as solvents, keeping the geometry optimized for the isolated species (single-point calculations).

Results and discussion

Neutral $\text{Cp}_2\text{Fe}_2\text{S}_4$ complex

The geometry of the neutral complex was first studied with the $(\mu\text{-}\eta^1\text{-S}_2, \mu\text{-}\eta^2\text{-S}_2)$ coordination mode of the bridging S_2 units, as found experimentally for the major isomer (A) of the complex. Optimization was performed within the C_{2v} symmetry constraint, that is with eclipsed cyclopentadienyl ligands, as found for the experimental structure with unsubstituted Cp ligands.^{11,12} The optimized structure (I), shown in Fig. 2, was further characterized as a minimum on the potential energy surface. The main theoretical parameters are reported in Table 1 together with the experimental ones.¹² On the whole, the agreement between theoretical and experimental values is satisfactory. The Fe–S distances are overestimated by 0.039 and 0.050 Å (mean values) for the $\mu\text{-}\eta^1$ and the $\mu\text{-}\eta^2$ bonding modes, respectively. In agreement with the experimental trend, the former is found to be significantly

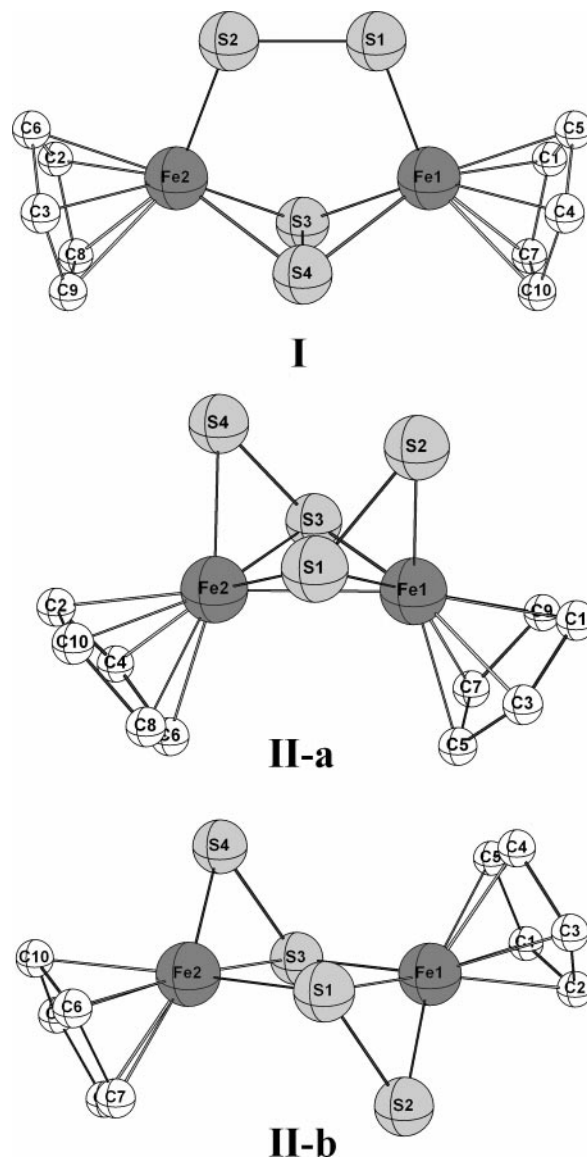


Fig. 2 Optimized structures of the neutral complexes $\text{Cp}_2\text{Fe}_2(\mu\text{-}\eta^1\text{-S}_2)(\mu\text{-}\eta^2\text{-S}_2)$ (I) and $\text{Cp}_2\text{Fe}_2[\mu\text{-(}\eta^1, \eta^2\text{)-S}_2]_2$ with either *syn* (II-a) or *anti* (II-b) positions of the S_2 units. Hydrogen atoms of the cyclopentadienyl ligands are omitted for clarity.

shorter than the latter, by 0.167 Å [expt.: 0.155 Å (mean values)]. Deviations in the same range are found for the S–S distances which are overestimated by 0.022 and 0.063 Å for the $\eta^1\text{-S}_2$ and the $\eta^2\text{-S}_2$ units, respectively. The S–S bond

Table 1 Main geometrical parameters optimized for the $\text{Cp}_2\text{Fe}_2(\mu\text{-}\eta^1\text{-S}_2)(\mu\text{-}\eta^2\text{-S}_2)$ complex (I, Fig. 2) and for the *syn* (II-a, Fig. 2) and the *anti* (II-b, Fig. 2) isomers of the $\text{Cp}_2\text{Fe}_2[\mu\text{-(}\eta^1, \eta^2\text{)-S}_2]_2$ complex. Distances are in Å and angles in °

	A (expt.) ^a	I	B (expt.) ^a	II-a	II-b
Fe–S1(1,2)(avg.)	2.105(6) ^b	2.144	2.209(2)	2.240	2.392
Fe1–S3	2.260(6) ^b	2.311	2.183(2)	2.232	2.279
S1–S2	1.999(8)	2.021	2.022(3)	2.055	2.084
S4–S3	2.044(8)	2.107	2.022(3)	2.055	2.084
Fe1...Fe2	3.494	3.539	2.650(2)	2.630	3.469
Fe–C ^b	2.08(1)	2.165	2.085(9)	2.155	2.163
S1–Fe1–S3	98.6(2) ^b	98.8	97.4(1)	98.9	84.1
Fe1–S1–S2	110.8(3) ^b	110.7	64.6(1)	65.0	57.5
Fe2–S4–S3	63.1(2) ^b	62.9	61.7(1)	61.4	68.4
Fe1–S3–Fe2	101.1(2) ^b	100.0	74.2(1)	71.9	95.9
Energy/kcal mol ^{–1} ^c	—	0.0	—	5.1	25.2

^a Experimental parameters are taken from ref. 12. ^b Mean values. ^c The total energy in hartrees of reference I is –674.423 632.

length is shorter for the $\mu\text{-}\eta^1$ than for the $\mu\text{-}\eta^2$ coordination mode, by 0.086 Å [expt.: 0.045(8) Å]. The very long Fe \cdots Fe distance, which rules out any metal–metal bonding interaction, is well reproduced [3.539 instead of 3.494 Å (expt.)] while the mean Fe–C distance is overestimated by 0.085 Å. Note, however, the large uncertainty on the experimental value. Finally, the difference between theoretical and experimental values for the bond angles is always found to be less than 1°.

It is noteworthy that the X-ray structures of the complexes with Cp and Cp* ligands exhibit eclipsed^{11,12} and staggered¹³ conformations of the cyclopentadienyl ligands, respectively. The conformation in which the Cp ligands are staggered (C_s symmetry) was thus also optimized. The geometrical parameters were found to be almost identical to those reported in Table 1 and the characterization led to a single imaginary frequency of only 3i cm⁻¹ located on the cyclopentadienyl ligands. Furthermore, the energy difference between the staggered and the eclipsed conformers is less than 0.1 kcal mol⁻¹. This essentially free rotation of the Cp ligands is in agreement with the single Cp resonance observed in the ¹H NMR spectrum of the Cp₂Fe₂S₄ complex.¹²

The characterization of complex **I** led to a value of 509 cm⁻¹ for the vibration of the S₂ unit coordinated in a $\mu\text{-}\eta^2$ fashion, in good agreement with the value of 502 cm⁻¹ reported for the $\nu(\text{S-S})$ frequency in the complex with Cp* ligands.¹³ On the other hand, the vibration of the $\mu\text{-}\eta^1\text{-S}_2$ unit was found to be coupled with a vibration on the cyclopentadienyl ligands. Two vibrations in which this $\mu\text{-}\eta^1\text{-S}_2$ unit is involved were thus found, with frequencies equal to 566 and 580 cm⁻¹.

A second isomer was then studied in which each S₂ unit binds one metal center in a η^1 fashion and the other metal in a η^2 mode; this is the $\mu\text{-(}\eta^1, \eta^2\text{)}$ binding mode found in the minor isomer (**B**) of the Cp₂Fe₂S₄ complex.¹² Two structures were actually optimized which differ by the relative positions of the S₂ units, *syn* (**II-a**) or *anti* (**II-b**) (Fig. 2). Note that only the former has been characterized by X-ray crystallography, although the existence of the *anti* isomer in the isomerization reaction **I** → **II** was not excluded by the authors.¹² The Cp ligands were kept in the eclipsed conformation in both **II-a** and **II-b**, leading to the C₂ and C_i symmetries, respectively. The main theoretical parameters are reported in Table 1 as well as the experimental values for the *syn* isomer,¹² the optimized structures being depicted in Fig. 2. Both **II-a** and **II-b** were characterized as minima on the potential energy surface. Comparison between theoretical and experimental parameters for the *syn* isomer (**II-a**) reveals deviations in the range of that found for complex **I**. The central Fe₂S₂ four-membered ring is found to be puckered, with a Fe₁–S₁–Fe₂–S₂ dihedral angle of 32°, and the Fe \cdots Fe distance is much shorter than that found in complex **I** (2.630 instead of 3.539 Å), in good agreement with the experimental trend (2.650 instead of 3.494 Å). This iron–iron distance is consistent with metal–metal bonding interaction in **II-a**. The main geometrical change in going from the *syn* to the *anti* isomer (**II-b**) is a flattening of the core Fe₂S₂ ring, which becomes planar. This results in an important lengthening of the Fe \cdots Fe distance, from 2.630 to 3.469 Å, which prevents any iron–iron bonding interaction in the *anti* isomer **II-b**. Finally, **II-a** was found to be 20.1 kcal mol⁻¹ more stable than **II-b**, a result that definitely rules out the formation of the *anti* isomer in the isomerization reaction **I** → **II**.

In the *syn* isomer, $\nu(\text{S-S})$ frequencies equal to 543 and 550 cm⁻¹ were computed for the antisymmetrical and symmetrical vibrations of the S₂ units, no experimental data being available for this isomer. On the other hand, the unknown *anti* isomer exhibits a frequency at 502 cm⁻¹ for the antisymmetrical vibration of the S₂ units. Comparison with the values calculated for isomer **I** (between 509 and 580 cm⁻¹) confirms that the $\nu(\text{S-S})$ frequencies are not very sensitive to

the coordination mode of the S₂ units [$\mu\text{-}\eta^2$, $\mu\text{-}\eta^1$ or $\mu\text{-(}\eta^1, \eta^2\text{)}$].³³

From an energetic point of view, structure **I** was found to be more stable than structure **II-a** by 5.0 kcal mol⁻¹. Taking into account the solvent leaves this value almost unchanged (5.8 kcal mol⁻¹ for THF). Single-point energy-only calculations with polarization functions added to the metal double- ζ basis set³⁴ and to the carbon atoms³⁵ did not significantly modify this result (4.7 kcal mol⁻¹). Finally, we made use of the broken-symmetry approach proposed by Noodleman,³⁶ which has been recently successfully applied to binuclear compounds.^{37,38} An energy difference of 5.2 kcal mol⁻¹ was found between the two isomers (single-point calculations).³⁹ Whatever the level of calculation, the theoretical energy ordering is consistent with the fact that **I** is the major isomer and **II-a** the minor isomer in the Cp₂Fe₂S₄ experimental complex. However, the computed energy difference is too large with respect to the experimental ratio of the two isomers (63 : 37 in THF).¹¹

Dicationic [Cp₂Fe₂S₄]²⁺ complex

The geometry of the dicationic [Cp₂Fe₂(S₂)₂]²⁺ complex was studied with an η^2 coordination mode for each S₂ unit, that is, the structure found for the related experimental complex with Cp* ligands.^{14,15} The Cp ligands being kept staggered, geometry optimization was performed within the C_{2h} symmetry constraint. The main theoretical parameters are given in Table 2, together with the experimental ones. The optimized structure (**III**), pictured in Fig. 3, was further characterized as a minimum, neglecting two imaginary frequencies of 15i and 10i cm⁻¹ located on the cyclopentadienyl ligands.

As for the neutral complex, the Fe–S and S–S bond lengths are overestimated by about 0.05 Å and the bond angle values reproduced with an error smaller than 1°. The Fe \cdots Fe distance of 2.906 Å (expt.: 2.857 Å) is intermediate between that found for the major (**I**, 3.494 Å) and the minor (**II-a**, 2.650 Å) isomers of the neutral complex. It is sufficiently long to suggest the absence of an Fe–Fe bond in the dication, as expected for this 36-electron species. A value of 579 cm⁻¹ was found for the antisymmetrical vibration of the S₂ units, in good agreement with the experimental data (542 cm⁻¹).¹⁴ This value is larger than that computed for the $\eta^2\text{-S}_2$ unit in the neutral complex **I** (509 cm⁻¹), the S–S distance being actually shorter in the dication by 0.074 Å (expt.: 0.061 Å, Tables 1 and 2). Finally, this structure was reoptimized keeping the Cp ligands in an eclipsed conformation (C_{2v} symmetry). Almost identical geometrical parameters were found, the energy difference being less than 0.01 kcal mol⁻¹.

Table 2 Main geometrical parameters optimized for the [Cp₂Fe₂S₄]²⁺ dicationic complex (Fig. 3). Distances are in Å and angles in °

	Expt. ^a	III	IV
Fe1–S1	2.282(1)	2.338	2.073
Fe1–S2	2.283(1)	2.333	3.420
Fe1–S3	2.276(1)	2.333	2.348
Fe1–S4	2.288(1)	2.338	2.348
S1–S2	1.983(1)	2.033	2.115
Fe1 \cdots Fe2	2.857(1)	2.906	3.499
Fe–C ^b	2.10(3)	2.163	2.193
S3–Fe1–S4	51.51(3)	51.58	51.39
S1–Fe1–S4	80.63(3)	81.12	103.26
Fe1–S1–S2	64.27(3)	64.08	109.50
Fe1–S3–S4	64.54(3)	64.33	64.30
Fe1–S4–S3	63.95(3)	64.08	64.30
Fe1–S1–S2–Fe2	88.04(3)	–87.41	0.00
Energy ^c /kcal mol ⁻¹	—	0.0	35.0

^a Experimental parameters are taken from ref. 14. ^b Mean values.

^c The total energy in hartrees of reference **III** is –673.817 048.

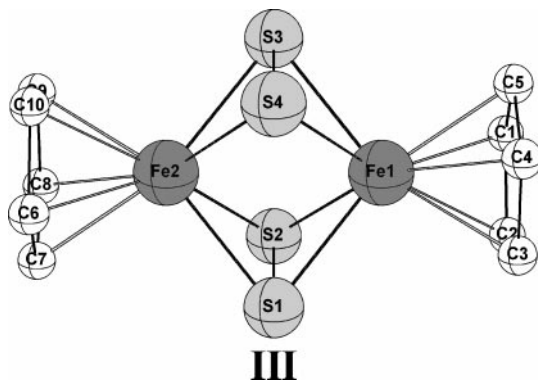


Fig. 3 Optimized structure of the dicationic complex $\text{Cp}_2\text{Fe}_2(\mu\text{-}\eta^2\text{-S}_2)_2^{2+}$ (**III**). Hydrogen atoms of the cyclopentadienyl ligands are omitted for clarity.

Therefore, the rotation of the Cp ligands is free in the dicationic complex **III**, as was found for the neutral species.

Starting from the geometry of the neutral complex (**I**), a second stationary point was located on the potential energy surface of the dication (structure **IV**, Table 2). Its geometry resembles that of **I**, with one S_2 unit coordinated in an η^1 fashion and the other η^2 (Fig. 2). Structure **IV** (a 32-electron species) was, however, found to be $35.0 \text{ kcal mol}^{-1}$ less stable than structure **III** and was further characterized as a transition state. The imaginary frequency of $70i \text{ cm}^{-1}$ is associated with the rotation of the $\eta^1\text{-S}_2$ ligand around the C_2 axis ($\eta^1\text{-S}_2 \rightarrow \eta^2\text{-S}_2$) so that this transition state connects two equivalent structures of the minimum depicted in Fig. 3. Finally, we failed to find a stationary point in a geometry close to that optimized for the minor isomer of the neutral complex (**II-a**), with an (η^1, η^2) coordination of both S_2 units: geometry optimization starting from this geometry collapses to the minimum energy structure **III**.

Monocationic $[\text{Cp}_2\text{Fe}_2\text{S}_4]^+$ complex

Cyclic voltammetry experiments on $\text{Cp}^*\text{Fe}_2\text{S}_4$ have shown that the two-electron oxidation of **I** leading to the dication **III** is a two-step process that involves first the intermediate formation of the monocation.^{14,15} Although the experimental structure of the monocation is not known, the quasi-reversibility of this first step suggested that no significant ligand reorientation occurs at this stage of the oxidation process. The structure of the monocation was then first optimized starting from the geometry of the neutral complex **I**. A stationary point (**V**), in which the $(\eta^1\text{-S}_2)(\eta^2\text{-S}_2)$ coordination modes are preserved, was located and characterized as a minimum. Its structure is pictured in Fig. 4 and the main geometrical parameters are reported in Table 3. A second minimum (**VI**, Fig. 4 and Table 3) was found starting from the

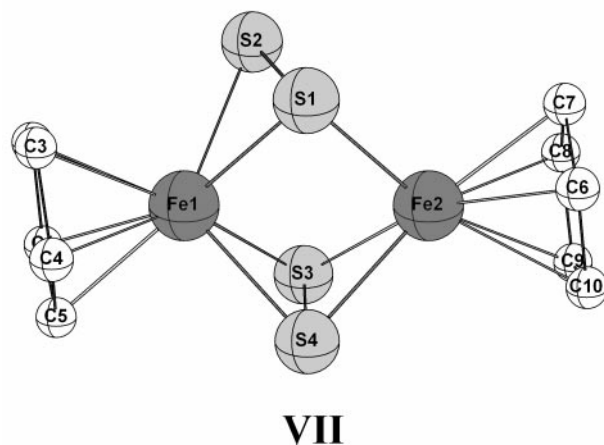
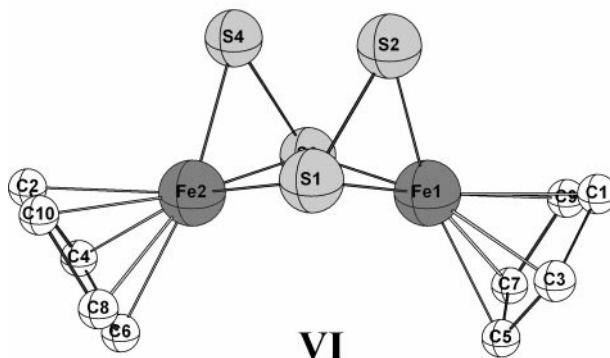
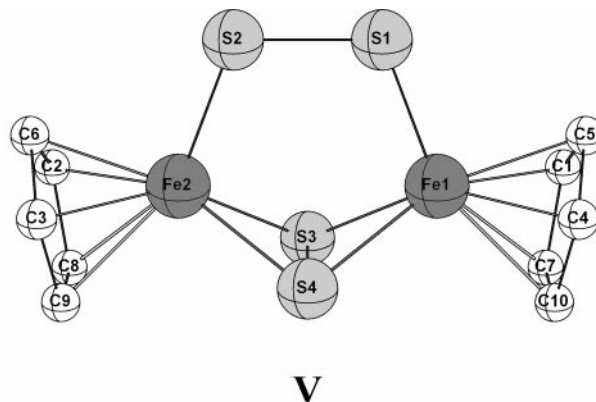


Fig. 4 Optimized structures (minima) of the monocationic complex with $(\mu\text{-}\eta^1\text{-S}_2)(\mu\text{-}\eta^2\text{-S}_2)$ (**V**), $[\mu\text{-}(\eta^1, \eta^2)\text{-S}_2]_2$ (**VI**) and $(\mu\text{-}\eta^2\text{-S}_2)(\mu\text{-}\eta^1, \eta^2)\text{-S}_2$ (**VII**) coordination modes for the bridging S_2 units. Hydrogen atoms of the cyclopentadienyl ligands are omitted for clarity.

Table 3 Main geometrical parameters optimized for the $[\text{Cp}_2\text{Fe}_2\text{S}_4]^+$ monocationic complex (Fig. 4). Distances are in Å and angles in $^\circ$.

	V	VI	VII
Fe1–S1	2.209	2.327	2.309
Fe1–S3	2.343	2.351	2.324
S1–S2	2.020	2.079	2.055
S3–S4	2.081	2.079	2.065
Fe1...Fe2	3.555	3.128	3.085
Fe–C ^a	2.195	2.188	2.161
S1–Fe1–S3	100.57	93.40	96.65
S2–S1–Fe1	110.33	62.85	64.87
Fe1–S3–Fe2	98.68	83.93	81.99
Energy/kcal mol ^{−1b}	0.0	11.0	4.2

^a Mean values. ^b The total energy in hartrees of reference **V** is $-674.204\,056$.

geometry of the neutral complex **II-a** with (η^1, η^2) coordination of each S_2 unit. Its energy was, however, $11.0 \text{ kcal mol}^{-1}$ above that of structure **V**. Finally, using the geometry of the dication (**III**) as a starting point, a third minimum was characterized (**VII**, Fig. 4 and Table 3) in which the S_2 ligands are coordinated in η^2 and (η^1, η^2) fashions, respectively. Its energy is only $4.2 \text{ kcal mol}^{-1}$ higher than that of structure **V**. The optimized Fe...Fe distances (3.555 , 3.132 and 3.085 Å for structures **V**, **VI** and **VII**, respectively) suggest there is no bonding interaction between the metal centers in the monocationic complex.

The most stable structure found for the monocation is thus that in which the coordination mode of the S_2 ligands is as for the major isomer of the neutral complex, as was suggested by the cyclic voltammetry experiments. On the other hand, it has been shown experimentally that there is a disproportionation pathway for the generation of the neutral and the dicationic

species from the monocationic one.^{14,15} It is often believed that such a reaction takes place when two different forms of the monocation are involved, one resembling the neutral complex, the other the dicationic one. In this respect, it is noteworthy that the lowest energy structure **V** resembles that of the neutral complex (major isomer) while the coordination mode in structure **VII** [$(\eta^2\text{-S}_2)(\eta^1, \eta^2)\text{-S}_2$] is intermediate between that found for the neutral (**I**) and the dicationic (**III**) species. Therefore, structures **V** and **VII** of the monocation might be candidates for the disproportionation reaction. The energetics are, however, very unfavorable in the gas phase ($\Delta E = 100.8 \text{ kcal mol}^{-1}$), a value that is significantly lowered by taking into account the solvation energies of the species involved in that reaction ($\Delta G = 39.6$ and $33.2 \text{ kcal mol}^{-1}$ in CH_2Cl_2 and CH_3CN , respectively).

Dianionic $[\text{Cp}_2\text{Fe}_2\text{S}_4]^{2-}$ complex

An irreversible two-electron reduction of the neutral complex has been observed in cyclic voltammetry experiments,^{11,12,15} but the structure of the dianion is still unknown. We first studied this species in the structure experimentally characterized for the isoelectronic $\text{Cp}_2\text{Co}_2\text{S}_4$ complex,¹³ in which the anti S_2 bridging ligands are both coordinated in a (η^1, η^2) manner (36-electron species). Two isomers were optimized, with the S_2 units either in *anti* (**VIII-a**) or *syn* (**VIII-b**) position (Table 4 and Fig. 5). In the former, the Fe_2S_2 core is essentially planar, with a $\text{Fe}\cdots\text{Fe}$ distance of 3.454 \AA , while it is slightly puckered in the latter, leading to a shortening of the iron–iron distance (3.390 \AA). Both these structures were further characterized as minima on the potential energy surface, the *anti* isomer being found to be more stable than the *syn* isomer by $7.8 \text{ kcal mol}^{-1}$, a result in agreement with the structure of the isoelectronic $\text{Cp}_2\text{Co}_2\text{S}_4$ complex.¹³ Two other optimizations were performed starting from structures **I** and **II-a** of the neutral complex. The former led to a new minimum (**IX**, Table 4 and Fig. 5), in which the $(\eta^1\text{-S}_2)(\eta^2\text{-S}_2)$ coordination mode is retained, its energy being $12.9 \text{ kcal mol}^{-1}$ above that of **VIII-a**. Not surprisingly, the optimization starting from the geometry of **II-a** collapses to the structure **VIII-b** already characterized as a minimum on the potential energy surface.

It has been suggested that the formation of the dianion from the neutral species might be accompanied by a cleavage of the S-S bond in the $\eta^2\text{-S}_2$ ligand,¹⁵ as already observed in the two-electron reduction of $\text{Fe}_2(\text{CO})_6\text{S}_2$.⁴⁰ Optimization of this structure (a 34-electron species), with two bridging sulfur ligands, actually led to a new minimum **X**, (Table 4 and Fig. 5) whose formation can, however, be excluded on energetic grounds ($23.0 \text{ kcal mol}^{-1}$ above **VIII-a**). In conclusion, the most stable structure for the dianionic $[\text{Fe}_2\text{Cp}_2\text{S}_4]^{2-}$ complex was found to be similar to that of the isoelectronic neutral

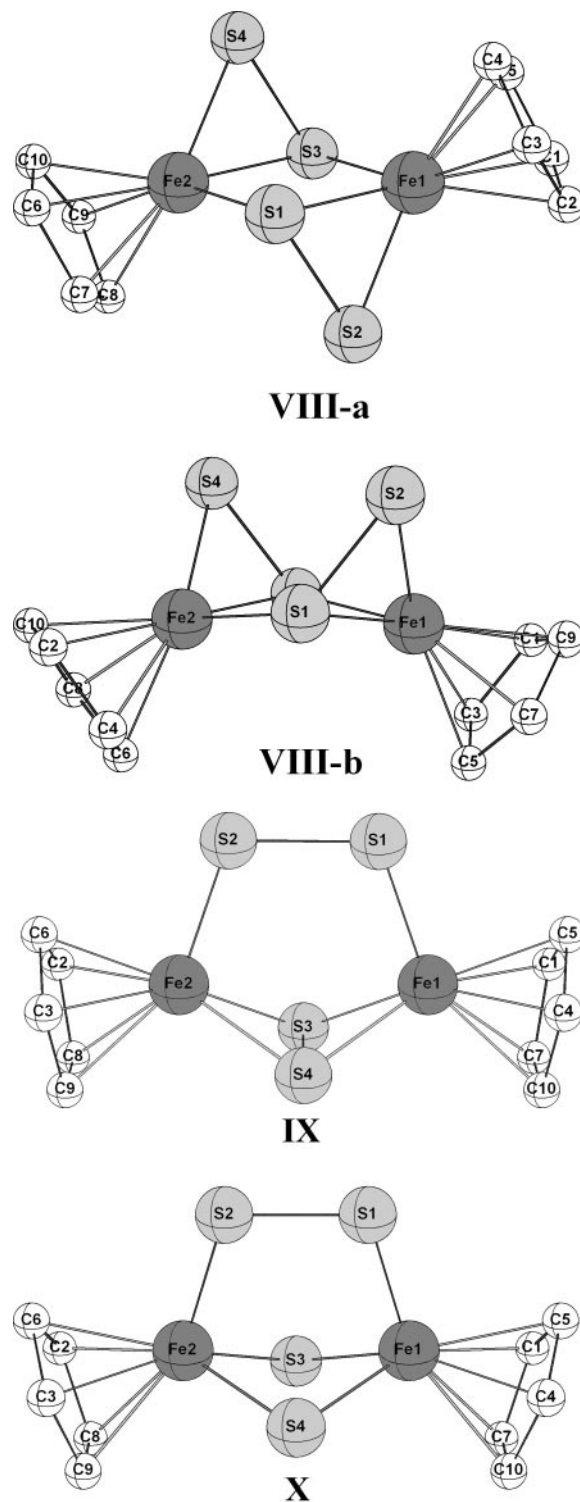


Fig. 5 Optimized structures (minima) of the dianionic complex with $[\mu\text{-(}\eta^1, \eta^2\text{)-S}_2]_2$ (**VIII-a**, *anti* isomer **VIII-b**, *syn* isomer), $(\mu\text{-}\eta^1\text{-S}_2)(\mu\text{-}\eta^2\text{-S}_2)$ (**IX**) and $(\mu\text{-}\eta^1\text{-S}_2)(\mu\text{-S})_2$ (**X**) coordination modes for the bridging sulfurs. Hydrogen atoms of the cyclopentadienyl ligands are omitted for clarity.

cobalt complex, in which the anti S_2 units are both coordinated in a $\mu\text{-(}\eta^1, \eta^2\text{)}$ manner (**VIII-a**).

Solvation energies and redox potentials

In order to study the energetics of the redox processes in which charged species are generated, solvent effects were introduced in the calculations. We are aware of the difficulty of such calculations in large systems with transition metal atoms, and that only semi-quantitative results can be

Table 4 Main geometrical parameters optimized for the $[\text{Cp}_2\text{Fe}_2\text{S}_4]^{2-}$ dianionic complex (Fig. 5). Distances are in \AA and angles in $^\circ$.

	VIII-a	VIII-b	IX	X
Fe1–S1	2.336	2.343	2.316	2.147
Fe1–S3	2.325	2.360	2.368	2.339
S1–S2	2.154	2.140	2.161	2.046
S3–S4	2.154	2.140	2.144	3.054
Fe1 \cdots Fe2	3.454	3.390	3.672	3.293
Fe–C ^a	2.217	2.213	2.233	2.257
S1–Fe1–S3	84.37	86.30	99.41	93.64
S2–S1–Fe1	63.40	62.63	109.05	106.88
Fe1–S3–Fe2	95.63	92.26	101.66	89.49
Energy ^b /kcal mol ^{−1}	0.0	7.8	12.9	23.0

^a Mean values. ^b The total energy in hartrees of reference **VIII-a** is $-674.409\,621$.

Table 5 Solvation energies (ΔG_{sol}) of the neutral (I), monocationic (V), dicationic (III) and dianionic (VIII-a) species and free energy changes (ΔG_{ox}) associated with the various oxidation processes. Energies are given in kcal mol⁻¹

ΔG_{sol}	M	M ⁺	M ²⁺	M ²⁻
CH ₂ Cl ₂	-6.2	-35.9	-126.3	-124.4
CH ₃ CN	+3.2	-29.2	-129.2	-126.9
ΔG_{ox}	M → M ⁺	M ⁺ → M ²⁺	M ²⁻ → M	
Gas	137.8	242.8	-8.8	
CH ₂ Cl ₂	108.1	152.4	109.5	
CH ₃ CN	105.4	142.9	121.3	

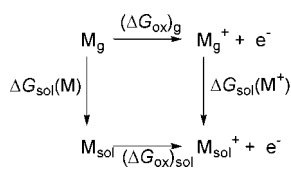
expected. Similar approaches can, however, be found in the recent literature.^{21,41}

Solvation energies were first computed by means of single-point PCM calculations on the most stable structures of the neutral (I), monocationic (V), dicationic (III) and dianionic (VIII-a) species with acetonitrile and dichloromethane as solvents (Table 5). The solvation free energies (ΔG_{sol}) calculated for the neutral complex are -6.2 and +3.2 kcal mol⁻¹ in CH₂Cl₂ and CH₃CN, respectively. The latter value is surprisingly found to be positive, but it is very small, in the range of the uncertainties expected for such single-point calculations. Charged species are expected to be more sensitive to the influence of polar solvents. Solvation energies in the range of -30 and -125 kcal mol⁻¹ are actually found for the monocation and the doubly charged species (dication and dianion), respectively (Table 5). According to a thermodynamic cycle such as that given in Scheme 1, the free energy changes associated with the oxidation reactions M → M⁺, M⁺ → M²⁺ and M²⁻ → M in the solvent ($\Delta G_{\text{ox}}^{\text{sol}}$) can be deduced from the values calculated in the gas phase ($\Delta G_{\text{ox}}^{\text{g}}$) and the solvation energies of the species involved in the various ionization processes. Theoretical values of ($\Delta G_{\text{ox}}^{\text{g}}$) and ($\Delta G_{\text{ox}}^{\text{sol}}$) are reported in Table 5. Owing to the large solvation energies, dramatic changes in the ΔG s were found upon going from the gas phase to the solution, in particular when doubly charged species are involved (decrease by 90–100 kcal mol⁻¹ for the monocation → dication reaction and increase by 120–130 kcal mol⁻¹ for the dianion → neutral reaction). Note that the spontaneous character of the double ionization of the dianion found in the gas phase ($\Delta G_{\text{ox}} = -8.8$ kcal mol⁻¹) disappears in solution ($\Delta G_{\text{ox}} = 109.5$ and 121.3 kcal mol⁻¹ in CH₂Cl₂ and CH₃CN, respectively).

Redox potentials can now be evaluated from these results. The free energy associated with the oxidation process M → Mⁿ⁺ can be expressed as follows:

$$(\Delta G_{\text{ox}}^{\text{sol}})(\text{M} \rightarrow \text{M}^{n+}) = nFE_{\text{abs}}(\text{M}^{n+}/\text{M})$$

with $F = 96\,500$ C and E_{abs} the absolute redox potential, being the potential that uses the vacuum state as its zero. In order to compare the calculations with the experimental results, the theoretical value must be referenced to the standard hydrogen electrode by adding a known constant potential ($\Delta \text{SHE} = -4.43$ V).⁴² Calculated and available experimental redox potentials (vs. NHE) in dichloromethane and acetonitrile are reported in Table 6, together with the values derived from the calculated gas-phase energies. Accord-



Scheme 1

Table 6 Calculated and experimental redox potentials (in V) vs. NHE in CH₂Cl₂ and CH₃CN. Calculated gas-phase values are also reported for comparison

	Gas	CH ₂ Cl ₂		CH ₃ CN	
		Calc.	Expt. ^a	Calc.	Expt. ^{a,b}
M ⁺ /M	+1.54	+0.25	+0.50	+0.13	+0.81, ^b 0.47 ^a
M ²⁺ /M ⁺	+6.09	+2.17	+1.49	+1.76	0.92 ^a
M/M ²⁻	-4.62	-2.06	-0.98	-1.80	-0.93 ^b

^a M = Fe₂(Cp*)₂S₄ (ref. 15). ^b M = Fe₂Cp₂S₄ (ref. 11).

ing to the crudeness of our solvent calculations, the agreement is reasonably satisfactory with deviations ranging from 0.25 to 1.08 V. In any case, taking into account the solvent effects significantly improves the results, since the errors using gas-phase values were found to lie between 0.73 and 5.17 V.

Summary

Calculated values for the neutral Cp₂Fe₂S₄ complex (two isomers) and its dication are found to be in good agreement with the experimental data (X-ray). Geometry optimization of the monocationic and the dianionic species (unknown experimentally) leads to several minima. The most stable involve the (μ-η¹)(μ-η²) and the 2(μ-η¹,η²) coordination modes of the S₂ units for the monocation and the dianion, respectively. Finally, redox potentials for the M⁺/M, M²⁺/M⁺ and M/M²⁻ couples are calculated using CH₂Cl₂ and CH₃CN as solvents (PCM). Deviations from 0.25 to 1.08 V are found between theoretical and experimental values.

Acknowledgements

The use of computational facilities of the Institut du Développement et des Ressources en Informatique Scientifique (IDRIS, Project No. 1269) (S. B., I. D. and Y. J.) and of the Centre de Supercomputació i Comunicacions de Catalunya (C⁴) (A. L.) are gratefully appreciated. S. B. thanks the EU and CESA/CEPBA for sponsoring her visit to the UAB under the Improving Human Potential program (HPRI CT 1999 00071). A. L. acknowledges financial support from the Spanish DGESIC (PB98 0916 CO2 01). L. Nadjo is thanked for helpful discussions.

References and notes

- J. Wachter, *Angew. Chem., Int. Ed. Engl.*, 1989, **28**, 1613.
- H. Ogino, S. Inomata and H. Tobita, *Chem. Rev.*, 1998, **98**, 2093.
- (a) R. H. Holm, *Adv. Inorg. Chem.*, 1992, **38**, 1; (b) M. Hidai, S. Kuwata and Y. Mizobe, *Acc. Chem. Res.*, 2000, **33**, 46.
- P. J. Lundmark, G. J. Kubas and B. L. Scott, *Organometallics*, 1996, **15**, 3631.
- C. M. Bolinger, T. B. Rauchfuss and A. L. Rheingold, *J. Am. Chem. Soc.*, 1983, **105**, 6321.
- L. Y. Goh and T. C. W. Mak, *J. Chem. Soc., Chem. Commun.*, 1986, 1474.
- M. Rakowski DuBois, D. L. DuBois, M. C. VanDerveer and R. C. Haltiwanger, *Inorg. Chem.*, 1981, **20**, 3064.
- A. E. Bruce and D. R. Tyler, *Inorg. Chem.*, 1984, **23**, 3433.
- H. Brunner, W. Meier, J. Wachter, E. Guggolz, T. Zahn and M. L. Ziegler, *Organometallics*, 1982, **1**, 1107.
- H. Chaunaud, A. M. Ducourant and C. Giannotti, *J. Organomet. Chem.*, 1980, **190**, 201.
- R. Weberg, R. C. Haltiwanger and M. Rakowski DuBois, *Organometallics*, 1985, **4**, 1315.
- R. Weberg, R. C. Haltiwanger and M. Rakowski DuBois, *New J. Chem.*, 1988, **12**, 361.
- H. Brunner, N. Janietz, W. Meier, G. Sergeson, J. Watcher, T. Zahn and M. L. Ziegler, *Angew. Chem., Int. Ed. Engl.*, 1985, **24**, 1060.
- H. Ogino, H. Tobita, S. Inomata and M. Shimoi, *J. Chem. Soc., Chem. Commun.*, 1988, 586.

- 15 H. Brunner, A. Mertz, J. Pfauntsch, O. Serhadli, J. Watcher and M. L. Ziegler, *Inorg. Chem.*, 1988, **27**, 2055.
- 16 T. B. Rauchfuss, D. P. S. Rodgers and S. R. Wilson, *J. Am. Chem. Soc.*, 1986, **108**, 3114.
- 17 M. Yuki, K. Kuge, M. Okazaki, T. Mitsui, S. Inomata, H. Tobita and H. Ogino, *Inorg. Chim. Acta*, 1999, **291**, 395.
- 18 W. Tremel, R. Hoffmann and E. D. Jemmis, *Inorg. Chem.*, 1989, **28**, 1213.
- 19 (a) J. E. McGrady and R. Stranger, *J. Am. Chem. Soc.*, 1997, **119**, 8512; (b) P. E. M. Siegbahn and R. H. Crabtree, *J. Am. Chem. Soc.*, 1997, **119**, 3103; (c) T. C. Brunold, N. Tamura, K. Nobumasa, Y. Moro-oka and I. Solomon, *J. Am. Chem. Soc.*, 1998, **120**, 5674; (d) P. E. M. Siegbahn, *Inorg. Chem.*, 1999, **38**, 2880; (e) M. F. Flock and K. Pierloot, *J. Phys. Chem. A*, 1999, **103**, 95; (f) B. M. T. Lam, J. A. Halfen, V. G. Young, Jr., J. R. Hagadorn, P. L. Holland, A. Lledos, L. Cucurull-Sánchez, J. J. Novoa, S. Alvarez and W. B. Tolman, *Inorg. Chem.*, 2000, **39**, 4072.
- 20 J. E. McGrady and R. Stranger, *Inorg. Chem.*, 1999, **38**, 550.
- 21 (a) J.-M. Mouesca, J. L. Chen, L. Noodleman, D. Bashford and D. A. Case, *J. Am. Chem. Soc.*, 1994, **116**, 11898; (b) J. Li, M. R. Nelson, C. Y. Peng, D. Bashford and L. Noodleman, *J. Phys. Chem. A*, 1998, **102**, 6311.
- 22 M. J. Frisch, G. W. Trucks, H. B. Schlegel, G. E. Scuseria, M. A. Robb, J. R. Cheeseman, V. G. Zakrzewski, J. A. Montgomery, R. E. Stratmann, J. C. Burant, S. Dapprich, J. M. Millam, A. D. Daniels, K. N. Kudin, M. C. Strain, O. Farkas, J. Tomasi, V. Barone, M. Cossi, R. Cammi, B. Mennucci, C. Pomelli, C. Adamo, S. Clifford, J. Ochterski, G. A. Petersson, P. Y. Ayala, Q. Cui, K. Morokuma, D. K. Malick, A. D. Rabuck, K. Raghavachari, J. B. Foresman, J. Cioslowski, J. V. Ortiz, B. B. Stefanov, G. Liu, A. Liashenko, P. Piskorz, L. Komaromi, R. Gomperts, R. L. Martin, D. J. Fox, T. Keith, M. A. Al-Laham, C. J. Peng, A. Nanayakkara, C. Gonzalez, M. Challacombe, P. M. W. Gill, B. Johnson, W. Chen, M. W. Wong, J. L. Andres, C. Gonzalez, M. Head-Gordon, E. S. Replogle and J. A. Pople, GAUSSIAN 98 Rev. A.6, Gaussian, Inc., Pittsburgh PA, 1998.
- 23 R. G. Parr and W. Yang, *Density Functional Theory of Atoms and Molecules*, Oxford University Press, Oxford, UK, 1989.
- 24 T. Ziegler, *Chem. Rev.*, 1991, **91**, 651.
- 25 C. Lee, W. Yang and R. G. Parr, *Phys. Rev. B*, 1988, **37**, 785.
- 26 A. D. Becke, *J. Chem. Phys.*, 1993, **98**, 5648.
- 27 P. J. Stephens, F. J. Delvin, C. F. Chabalowski and M. J. Frisch, *J. Phys. Chem.*, 1994, **98**, 11623.
- 28 P. J. Hay and W. R. Wadt, *J. Chem. Phys.*, 1985, **82**, 299.
- 29 W. R. Wadt and P. J. Hay, *J. Chem. Phys.*, 1985, **82**, 284.
- 30 A. Höllwarth, M. Böhme, S. Dapprich, A. W. Ehlers, A. Gobbi, V. Jonas, K. F. Köhler, R. Stegman, A. Veldkamp and G. Frenking, *Chem. Phys. Lett.*, 1993, **208**, 237.
- 31 W. J. Hehre, R. Ditchfield and J. A. Pople, *J. Chem. Phys.*, 1972, **56**, 2257.
- 32 J. Tomasi and M. Persico, *Chem. Rev.*, 1994, **94**, 2027.
- 33 (a) A. Müller and E. Dieman, *Adv. Inorg. Chem.*, 1987, **31**, 89; (b) A. Müller, W. Jaegermann and J. H. Enemark, *Coord. Chem. Rev.*, 1982, **46**, 245.
- 34 A. W. Elhers, M. Böhme, S. Dapprich, A. Gobbi, A. Höllwarth, V. Jonas, K. F. Köhler, R. Stegman, A. Veldkamp and G. Frenking, *Chem. Phys. Lett.*, 1993, **208**, 111.
- 35 P. C. Hariharan and J. A. Pople, *Theor. Chim. Acta*, 1973, **28**, 213.
- 36 L. Noodleman, *J. Chem. Phys.*, 1981, **74**, 5737.
- 37 (a) E. Ruiz, J. Cano, S. Alvarez and P. Alemany, *J. Am. Chem. Soc.*, 1998, **120**, 11122; (b) C. Adamo, V. Barone, A. Bencini, F. Totti and I. Ciofini, *Inorg. Chem.*, 1999, **38**, 1996; (c) J. E. McGrady, R. Stranger and T. Lovell, *Inorg. Chem.*, 1998, **37**, 3802; (d) R. Stranger, J. E. McGrady and T. Lovell, *Inorg. Chem.*, 1998, **37**, 6795.
- 38 (a) A. Lledos and Y. Jean, *Chem. Phys. Lett.*, 1998, **287**, 243; (b) I. Demachy, A. Lledos and Y. Jean, *Chem. Phys. Lett.*, 1999, **303**, 621; (c) Y. Jean and A. Lledos, *Chem. Commun.*, 1998, 1443; (d) I. Demachy, A. Lledos and Y. Jean, *Inorg. Chem.*, 1999, **39**, 5443; (e) S. Blasco, I. Demachy, Y. Jean and A. Lledos, *Inorg. Chim. Acta*, 2000, **300–302**, 837.
- 39 The broken-symmetry calculation on the syn II-a isomer leads to total atomic spin densities of ± 0.93 on the iron atoms (most being associated with the d orbitals) and to a $\langle S^2 \rangle$ value of 0.81. These results reflect the localization of the spin-up and spin-down magnetic orbitals and suggests that the bonding interaction between the metal centers is weak despite the rather short Fe...Fe distance. Further studies on the metal-metal bonding strength in the II-a isomer are in progress.
- 40 D. Seyferth, R. S. Henderson and L.-C. Song, *Organometallics*, 1982, **1**, 125.
- 41 (a) H. M. Olsson and U. Ryde, *J. Biol. Inorg. Chem.*, 1999, **4**, 654; (b) J. Li, C. L. Fisher, R. Konecny, D. Bashford and L. Noodleman, *Inorg. Chem.*, 1999, **38**, 929; (c) M.-H. Baik, T. Ziegler and C. K. Schauer, *J. Am. Chem. Soc.*, 2000, **122**, 9143.
- 42 H. Reiss and A. Heller, *J. Phys. Chem.*, 1985, **89**, 4207.